

Organic Nanostructures for Next Generation Devices

Bearbeitet von
Katharina Al-Shamery, Horst-Günter Rubahn, Helmut Sitter

1. Auflage 2008. Buch. xix, 358 S. Hardcover
ISBN 978 3 540 71922 9
Format (B x L): 15,5 x 23,5 cm

[Weitere Fachgebiete > Physik, Astronomie > Thermodynamik > Festkörperphysik,
Kondensierte Materie](#)

Zu [Inhaltsverzeichnis](#)

schnell und portofrei erhältlich bei


DIE FACHBUCHHANDLUNG

Die Online-Fachbuchhandlung beck-shop.de ist spezialisiert auf Fachbücher, insbesondere Recht, Steuern und Wirtschaft. Im Sortiment finden Sie alle Medien (Bücher, Zeitschriften, CDs, eBooks, etc.) aller Verlage. Ergänzt wird das Programm durch Services wie Neuerscheinungsdienst oder Zusammenstellungen von Büchern zu Sonderpreisen. Der Shop führt mehr als 8 Millionen Produkte.

Fundamentals of Organic Film Growth and Characterisation

H. Sitter, R. Resel, G. Koller, M.G. Ramsey, A. Andreev, and C. Teichert

1.1 General

Currently, technical applications of organic nanoaggregates are discussed for various purposes like displays, electronic circuits, sensors and optical waveguides. In all these cases, the optical and electronic properties (and also the combination of both) are decisive parameters. Why are the structural properties of the nanoaggregates so important? The reason is the strong relationship between the structure (arrangement of the molecules within the bulk state) of the nanoaggregates and the application-relevant properties: optical emission and electronic charge transport.

The optical absorption and emission of organic molecules are highly polarised. Therefore, a strong optical anisotropy is observed for ordered bulk materials [1,2]. For example, in case of nanoneedles of the molecule sexiphenyl (or hexaphenyl) light with polarisation along the long molecular axes is emitted [3, 4]. Also the electronic charge transport shows anisotropic behaviour within an ordered bulk state [5]. It is generally accepted that the intermolecular charge transport happens along overlapping π -conjugated segments of neighbouring molecules [6,7]. Therefore, specific directions within an ordered bulk state show enhanced ability for charge transport.

Applications based on nanoaggregates which are prepared on surfaces are always associated with specific directions of light absorption/emission and charge transport. The orientation of the molecules as well as the directions of dense π -packing of neighbouring molecules are defined by the crystalline properties of the nanoaggregates. The orientation of the crystallites on the substrate surface is determined by the orientation of the molecules relative to the substrate surface. The alignment of the crystallites along specific surface directions is determined by the in-plane alignment of the molecules relative to the substrate.

One further important parameter for application is the size and shape of the crystalline domains. Generally, large single crystalline domains with regular shape are preferred. Grain boundaries disturb the regular lattice and

interrupt the periodic overlapping of neighbouring molecules, this considerably influences the charge transport [8,9].

1.2 Nucleation Process and Growth Modes

Each crystallisation process can be considered as a phase transition from a mobile phase into the solid phase of the crystal. In the case of layer growth the mobile phase, in our case the vapour is deposited on a solid surface. Consequently, an adsorption process is the first physical step in any deposition process. There are two types of adsorption. The first is physical adsorption, often called *physisorption*, which refers to the case where there is no electron transfer between the adsorbate and the substrate, and the attractive forces are van der Waals type. This type of adsorption is very typical for most of the organic molecules impinging on a substrate surface. The second type of adsorption is *chemisorption*, which refers to the case when electron transfer takes place between the adsorbate and the substrate, which means a chemical bond is formed. The forces are then of the type occurring in the appropriate chemical bond. This case is typical for the deposition of inorganic materials, which are usually at first physisorbed, undergo a dissociation process and are finally chemisorbed and incorporated into the growing crystal. In general, adsorption energies for physical adsorption are smaller than for chemical adsorption, which means that organic molecules are much weaker bound on the substrate in comparison to inorganic materials forming compounds.

It is experimentally well documented that thin films of organic and inorganic materials are formed by a “nucleation and growth” mechanism. Due to their growth, small clusters of atoms or molecules, so-called *nuclei*, are formed which further agglomerate to form islands. As growth proceeds, agglomeration increases, chains of islands are formed and eventually join up to produce a continuous deposit, which still can contain channels and holes. These holes eventually fill up to give a continuous and complete film and further growth leads to smoothening of the surface irregularities or in contrary these defects can be enhanced by further overgrowth. Consequently, understanding and controlling the process of layer formation by epitaxy implies in each case a detailed knowledge of the nucleation and growth modes.

Nucleation is the spontaneous formation of small embryonic clusters with a critical size determined by the equilibrium between their vapour pressure and the environmental pressure. The nuclei are formed in a metastable supersaturated or undercooled medium. Their appearance is a prerequisite for a macroscopic phase transition to take place. This means that nucleation is a precursor of the crystallisation process. Due to their increased surface/volume ratio, the critical clusters have more energy than the bulk phase of the same mass, hence they have a chance to survive and form a macroscopic entity of the new stable phase. Figure 1.1 shows the relationship between the vapour pressure of liquid droplets and their size [10]. If by any chance the critical

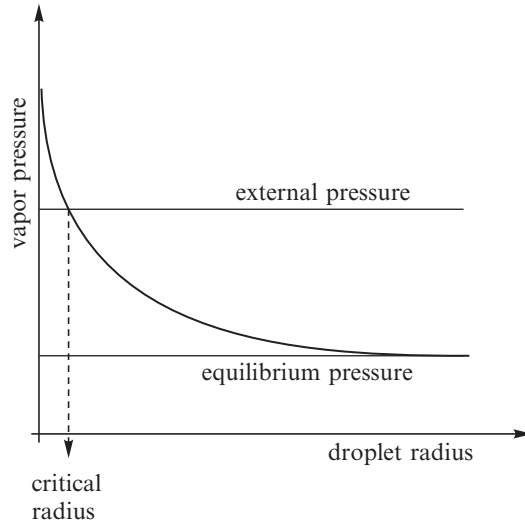


Fig. 1.1. Vapour pressure of small droplets in relation to their size (reprinted with permission from [10])

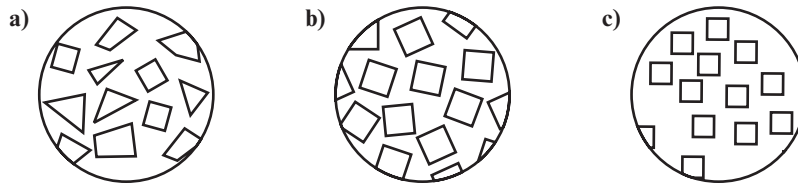


Fig. 1.2. Three intergrowth relations between deposit and substrate: (a) deposit is fully non-oriented, (b) texture orientation where the deposit planes are parallel to the substrate surface and (c) deposit exhibits texture and azimuthal orientation, a so-called epitaxial orientation to the substrate (reprinted with permission from [11])

radius of the droplet, defining its critical size, increases slightly, the droplet or cluster will continue to grow until a macroscopic two-phase equilibrium is attained. In the reverse case the droplet will disappear. This indicates that the energetics of layer formation is governed by the energetics of the critical nucleus.

Epitaxial nucleation is a special case of heterogeneous nucleation in which different kinds of intergrowth relations between the deposit and the substrate may occur. The orientation behaviour of the growing layer on a single crystalline substrate may not only be influenced by the nucleation process of the deposited material, but also by the subsequent growth on the substrate. In Fig. 1.2 three possible, basically different kinds of intergrowth relations between deposit and substrate are schematically shown [11].

According to Fig. 1.2a, the deposit crystallites are completely non-oriented with respect to the substrate crystal surface. As shown in Fig. 1.2b, an orientation of texture may exist, which means that all deposit crystallites grow with the same low index lattice plane on the substrate surface, however they are not oriented with respect to each other. Finally, as shown in Fig. 1.2c, the deposited crystallites and the substrate crystal show both the textural and azimuthal orientation towards one another. It should be emphasised that only these orientation relationship is designated as epitaxial.

Five different modes of crystal growth may be distinguished in epitaxy. These are the Volmer–Weber mode (VW-mode), the Frank–van der Merwe mode (FM-mode), the Stranski–Krastanov mode (SK-mode), the columnar growth mode (CG-mode) and the step flow mode (SF-mode) [12]. These five most frequently occurring modes are illustrated schematically in Fig. 1.3.

In the VW-mode, or island growth mode, small clusters are nucleated directly on the substrate surface and then grow into islands of the condensed phase. This happens when the molecules of the deposit are more strongly bound to each other than to the substrate. This mode is displayed by many systems growing on insulators like mica or organic substrates, because there are no unsaturated dangling bonds on the surface to form a strong bond between impinging molecules and the substrate. The FM-mode displays the opposite characteristics. Because the atoms or molecules are more strongly bound to the substrate than to each other, the first complete monolayer is formed on the surface, which becomes covered with a somewhat less tightly bound second layer. Providing that the decrease in binding strength is monotonic towards the value for the bulk material of the deposit, the layer growth mode is obtained. The SK-mode, or layer plus island growth mode, is an “intermediate” case. After forming the first monolayer, or a few monolayers, subsequent layer growth is unfavourable and islands are formed on top of this

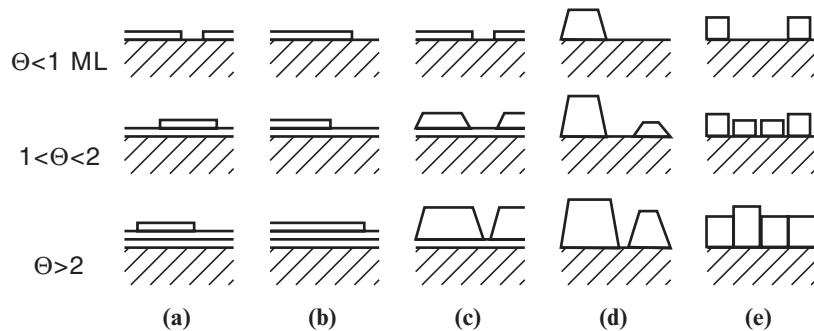


Fig. 1.3. Five crystal growth modes most frequently occurring on flat surfaces of substrate crystals: (a) layer-by-layer or Frank–van der Merwe, (b) step flow, (c) layer plus island or Stranski–Krastanov, (d) island or Volmer–Weber and (e) columnar growth mode. Θ represents the coverage in monolayers (reprinted with permission from [12])

intermediate layer. There are many possible reasons for this mode to occur and almost any factor which disturbs the monotonic decrease in binding energy characteristic for the layer-by-layer growth may be the cause. It occurs especially in cases when the interface energy is high (allowing for initial layer-by-layer growth) and the strain energy of the film is also high (making reduction of strain energy by islanding favourable).

The fifth mode, the CG-mode, shows some similarities with the SK- and VW-modes, however, it is fundamentally different. In the SK-mode as well as in VW-mode, with increasing thickness, the condensed islands tend to merge and cover the whole substrate surface. Although the grown film may exhibit variations in thickness and presence of structural defects at the interface where the islands merge, it forms a connected structure, in which the density of the film is homogeneous. In contrast, the films grown by CG-mode usually thicken without the merger of columns. As a result, columns usually remain separated throughout the growth process of the film, and the films grown in this mode are easily fractured. The CG-mode occurs where low surface mobility of the impinging molecules leads to the formation of columns of the deposited material.

Beside the described growth modes, the so-called *step flow growth mode* is observed on non-atomically flat substrate surfaces. That can occur, if the substrate surface contains cleaving steps or if the substrate is cut slightly misoriented from a low index plane, however the surface on the planes between the steps, the so-called *terraces*, is atomically flat. Two-dimensional nucleation may occur on the terraces, when the substrate temperature is sufficiently low, or the flux of the constituent molecules of the growing film is too high and therefore prohibits fast surface migration of the molecules. In this case the film may grow on the terraces in the FM- or SK-modes. However, if the substrate temperature is high enough or the flux is sufficiently low, then the impinging molecules can be mobile enough on the terraces that they become incorporated directly into the step edges. In this case, growth of the epitaxial film proceeds by the advancement of steps along the terraces.

1.3 The Surface Science Approach

The surface science approach involves in situ ultrahigh vacuum (UHV) growth on well defined and characterised generally single crystal substrates. The large variety of UHV surface science techniques available have been developed in the last 40 years, because of the needs of the inorganic semiconductor industry on the one hand and the aim to understand catalysis on the atomic/molecular level on the other hand. The blending of surface physics and chemistry into surface science provides the tools of both sciences and the interdisciplinary approach, appropriate for investigating organic semiconductor interfaces, structures and films.

Organic materials have a high propensity to crystallise, as the literature of sexiphenyl films grown on mica or the alkali halides illustrates, where numerous crystallite orientations, often co-existent, are reported (see Chap. 5; [13]). Despite the substrates being single crystals, this (unwanted) richness of organic structures is most likely due to the substrates being cleaved in air and is thus dependent on uncontrolled parameters such as the humidity of the day or the time it took to insert the sample into the growth chamber. The multi-technique approach and the controlled UHV experimental environment for both substrate and organic film preparation appear often rather slow and cumbersome, but the reader should bear in mind that: *You do not need UHV to fabricate organic structures, but you do need it to understand what is happening.*

1.3.1 In Situ UHV MBE

Moderately sized molecules, such as sexiphenyl, sexithiophene, pentacene and other oligomers as base materials for surface science studies, are available in the high purity required for controlled experiments. These can be evaporated from glass or metal crucibles, in a reproducible manner in UHV. Generally several days of thorough out-gassing in UHV are sufficient to purify the materials, here water is the principle problem, after which a background pressure in the 10^{-10} mbar range during evaporation is achievable. The latter is vital for reproducible experiments, particularly for more reactive substrates.

Despite the fact that many oligomers of interest have relatively low vapour pressures and are thus UHV compatible, care should be taken with evaporator design. There is a belief that the molecules “pump” and thus care need not be taken – this is a myth. They can coat chamber walls, etc., and lower the residence time of residual gases (in particular, water) and thus improve pumping rate and the system’s base pressure. In standard high vacuum device manufacturing chambers, this can lead to the partial pressures of residual gases being dependent on the chambers history. In UHV chambers, hot filaments in ion gauges, evaporators, sample heaters, etc., crack/desorb the molecules, leading to a partial pressure of molecular fragments, which makes controlled studies difficult. This is a particular problem one often faces in synchrotron end stations and other multiple user facilities. As a consequence, indiscriminate evaporation should be avoided and collimators to direct the evaporant should be used.

The propensity of the molecules to crystallise and grow three-dimensional nanostructures makes the use of surface-sensitive electron spectroscopies, such as X-ray photoemission (XPS) or Auger spectroscopy (AES), to quantify the amount of material applied very unreliable as they are area averaging techniques. Quartz microbalance measurements of the rate of evaporation are necessary. Here, quantities are quoted in equivalent film thicknesses assuming the bulk density of the evaporant. In surface science, a monolayer is defined as the number of adsorbate units equal to the number of substrate surface

atoms. It is used more loosely for the large organics as the amount of material required to coat the substrate with a single layer. As the molecules are extremely anisotropic, this varies from $\approx 3\text{--}4\text{ \AA}$ for a layer of lying molecules to $\approx 25\text{ \AA}$ for a monolayer of standing molecules, for the molecules and substrates considered here.

1.3.2 Valence Band Photoemission (ARUPS)

In photoelectron spectroscopy (PES), electrons are photoemitted by photons of energy $h\nu$ according to the photoelectric effect, and the kinetic energy of the photoelectrons is determined by the conservation law of energy following the modified Einstein relation $E_{\text{kin}} = h\nu - E_{\text{B}} - \phi$, where E_{B} is the binding energy of the electrons in the solid referenced to the Fermi level E_{F} and ϕ , the work function of the sample. As a result of the $h\nu$ dependence of the photoionisation cross-section ultraviolet (UV) photoelectron spectroscopy (UPS) is more suited to probe the valence electronic structure than X-ray photoelectron spectroscopy (XPS), which in turn is used to study core electron states. In addition to the energy, in angular-resolved UPS (ARUPS), the momentum of the photoelectron is measured, which can be related to the momentum of the electron in the solid. This allows the experimental determination of the electronic band structure of solids. Of particular relevance for ARUPS of molecular adsorbates are symmetry-derived polarisation-dependent selection rules for emissions in high symmetry directions of the adsorption complex. These selection rules can be derived from simple group theoretical arguments, and allow a qualitative symmetry analysis of ARUPS data [14–17].

With the example of benzene on Ni(110) in Fig. 1.4, the relationship between the UPS spectra of isolated molecules (gas phase) and those in adsorbed molecular monolayers and multilayer films is illustrated. In the measurement, the substrate and electron spectrometer are in thermodynamic equilibrium, and for the solid state the natural energy reference is the Fermi level (E_{F}). To facilitate comparison to the gas phase spectrum, the solid-state spectra have been referenced to the vacuum level (E_{vac}) by off-setting them by the work function as measured from the secondary electron cut-off in the UPS spectra [18]. In this case, the work function measured for both monolayer and condensed benzene multilayer is 4 eV and thus the Ni substrate Fermi edge is at 4 eV with respect to E_{vac} . In going from gas phase to the molecular solid, there is a rigid shift of all orbital emissions to lower binding energy (higher kinetic energy) due to the extra-molecular relaxation (Δ_{relax}); the electrons of neighbouring molecules are responding to the photohole and screening it. Between second and higher layers and the monolayer, there can be a further rigid shift to lower binding energy due to enhanced screening from the substrate. Additionally, the orbitals that are involved in the bonding to the substrate can have a differential shift to higher binding energy due to bond stabilisation. This is well expressed by the π orbitals involved in the benzene bond to Ni in Fig. 1.4. If, however, there is only an electrostatic bond to the substrate, as

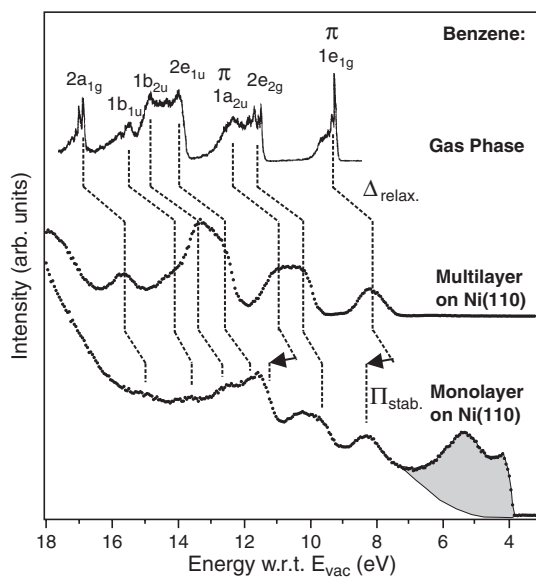


Fig. 1.4. Comparison of UPS spectra of benzene in the gas phase, a condensed film on Ni(110) and a benzene monolayer on Ni(110). The correlation between the orbitals in the three cases is indicated

for instance in the case of benzene on Al(111) [19], not only are no differential shifts observed, there is only a small shift due to substrate screening. Here the weaker bonding results in the molecules being further from the surface and its screening ability. For the larger π -conjugated molecules even when there is strong bonding to the substrate there is almost no screening shift between the monolayer and higher layers [20]. Presumably, the polarisability of the large conjugated systems such as sexiphenyl is as effective as the metal substrate in screening the photohole. Apart from the loss of vibrational fine structure, due to solid-state broadening, the spectral shape of the isolated molecule and the condensed film is very similar. In contrast, the monolayer is somewhat different as it is well ordered and photoemission selection rules are in play making the relative intensities of the orbital emissions very strongly with experimental geometry. To observe all orbitals and their energy positions correctly, spectra need to be taken in a variety of experimental geometries. For the smaller molecules, such as benzene these selection rules have often been exploited to determine the adsorbed molecules symmetry and thus the molecular geometry [17, 21]. As will be seen in Chap. 7, strong angular effects in the UPS spectra of monolayers and crystalline structures of the longer oligomers can be used to infer their orientation. A strict group theory selection rule analysis, however, is difficult due to the multiplicity of near degenerate orbitals in the larger molecules.

Figure 1.5 illustrates the development of the valence band structure with increasing chain length by comparing the UPS spectra from films of benzene,

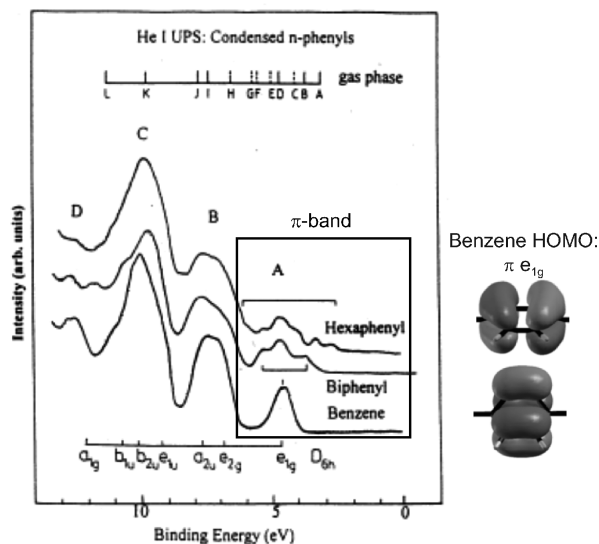


Fig. 1.5. Development of the valence band structure of n-phenyls with increasing chain length by comparing the spectra from films of benzene, biphenyl and sexiphenyl (reprinted with permission from [20])

biphenyl and sexiphenyl. It very clearly shows the development of the all important π band with oligomer length, while the appearance of the higher binding energy bands is essentially the same, as they are derived from intraring orbitals. The lowest binding energy emission of benzene results from the two degenerate π HOMO orbitals shown. In going to biphenyl the degeneracy is lifted, with two inter-ring bonding/anti-bonding pairs resulting. The pair of the first orbital has a high spatial overlap and consequently a large bonding/anti-bonding energy spread of almost 2 eV. The lower spatial overlap of the second results in a small energy separation of the two orbitals. In this seminal gas phase work on the dimer, Turner [22] called these the non-bonding orbitals. In angle-resolved UPS spectra of ordered films of biphenyl and bithiophene, these non-bonding orbitals can be distinguished and are seen to have an energy separation of 0.2–0.3 eV [23–25]. Increasing the oligomer length to sexiphenyl one sees the unresolved peak of the six near degenerate non-bonding π orbitals flanked by three anti-bonding and three bonding π orbitals, with the later merging into band B.

Photoemission requires conductive materials to avoid energy shifts due to charging. With the organics, high nanostructures, which can cause charging shifts, can form even at relatively moderate exposures. Both UV and X-ray radiation can also result in degradation of the molecules either directly or indirectly, via the secondary electrons from the substrate or, in the case of laboratory XPS, from the Al window of the source. The effect on the spectra can be subtle with cationic or anionic defects created effectively doping

the materials, leading to energy shifts and concomitant changes in the work function without significant degradation of the spectral fingerprint [26].

1.3.3 Near Edge X-Ray Absorption Fine Structure Spectroscopy (NEXAFS)

NEXAFS is a very versatile technique that can probe the orientation of molecular systems from sub-monolayer coverages to tens of nanometer thick films, if applied correctly [27,28]. In addition, given that NEXAFS probes the unoccupied molecular electronic states, one can determine changes of these, that may occur, e.g. due to charge transfer in the first layer bond or on doping [29].

The X-ray absorption near core level thresholds is measured via, for example, the yield of secondary or Auger electrons as a function of photon energy [30]. The core level excitations of highly oriented molecules exhibit a pronounced dependence on the light polarisation vector, with excitations of π^* and σ^* symmetry exhibiting opposite polarisation dependence.

Basic prerequisites for a correct interpretation of NEXAFS spectra include normalisation, background subtraction and a clear assignment of the molecular orbital symmetries (π^* or σ^*). A normalisation to the pre-absorption edge intensity is often appropriate. Background subtraction is particularly vital for films of sub-monolayer or monolayer coverage and can be done by either subtraction – or division – by a clean substrate spectrum or division by a simultaneously recorded gold reference spectrum [30]. To facilitate assigning the observed resonances of a NEXAFS spectrum, a simple model the so-called *building block principle* was proposed, which states that, due to the localisation of the excitation at the core hole position, one can describe larger molecules as a superposition of their smaller subunits, e.g. the larger oligomers should appear just as their monomers [30]. While often appropriate for non-conjugated molecules, it can no longer be applied for the conjugated molecules of organic electronics as illustrated in Fig. 1.6. Here the experimental data of thiophene oligomers, together with their corresponding density functional theory (DFT) calculations, illustrate how the carbon K-edge NEXAFS spectra become increasingly complex with increasing oligomer length [31]. The excellent agreement between experiment and theory should be noted, which allows a clear assignment of the orbital symmetries of complex molecules, such as the here displayed sexithiophene. In the top of Fig. 1.6, the azimuthal dependence of uniaxially oriented sexithiophene molecules grown on TiO_2 is shown: if the light polarisation is along the molecules, the π^* orbitals are all but invisible and the σ^* excitation is prominent, while for a polarisation across the molecules, the π^* orbitals are intense. Analysis of the π^* intensity as a function of X-ray incidence angle yields the average angle of the aromatic plane with respect to the substrate.

It is important to note that the measured signal in NEXAFS is an average over all molecules probed and thus one obtains the average orientation over the organic film surface to a depth from ≈ 20 Å to several hundred Ångstroms

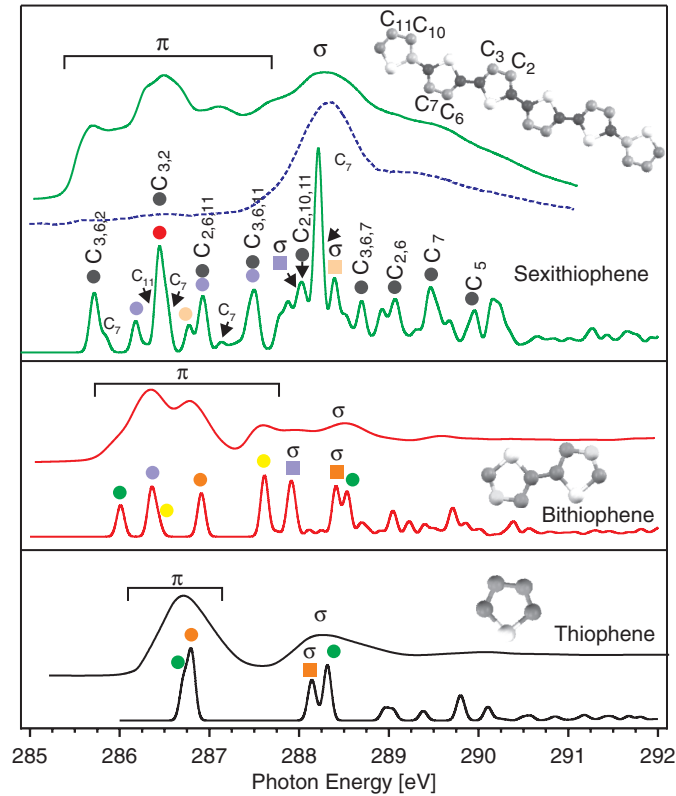


Fig. 1.6. DFT [31] calculated NEXAFS spectra (*bottom curves*) of thiophene, bithiophene and sexithiophene together with the experimental data. A rigid shift of 1.8 eV was applied to match the experiment. In the experimental geometry of the dashed spectrum of sexithiophene, only σ^* symmetric transitions are allowed

(depending on the detection method). This is in contrast to X-ray diffraction, where only molecules in a crystalline arrangement contribute to the signal. The unselective nature of NEXAFS is problematic for non-uniform films with several orientations, since NEXAFS will arrive at an average orientation. Or consider the case of inhomogeneous film growth, where starting from one particular molecular orientation, molecules with a second, different orientation continue to grow, here NEXAFS will wrongly suggest a gradual reorientation in the film. To unambiguously interpret NEXAFS results requires that either a NEXAFS resonance is forbidden for an experimental geometry, as for the sexithiophene example of Fig. 1.6, or the help of a second technique, here atomic force microscopy (AFM), is often quite useful for a first evaluation, as areas with different molecular orientation generally also differ in morphology. A number of synchrotron radiation end stations are being developed around the world that allow spatially resolved photoemission and absorption

spectroscopies, these will play an increasingly important role in the study of organic nanostructures [32].

1.3.4 Scanning Tunnelling Microscopy

The physical principle of the scanning tunnelling microscopy (STM) is the tunnelling current that can be established by applying an external bias voltage across a junction formed by a sharp metal tip brought in close proximity to a sample, so that the wave functions of sample and tip overlap. The magnitude of the tunnelling current depends exponentially on the distance, and by scanning the tip along the surface it can be used to obtain a topographical image of clean and adsorbate covered surfaces with atomic resolution. An example is shown in Fig. 1.7, where the exceptional resolution allows to determine the adsorption site of sexiphenyl on an oxygen-reconstructed Ni(110) surface. For the molecule shown, all six phenyl rings are centred on fourfold hollow positions of the underlying nickel atoms [33]. Such clear determination of the molecular registry is only rarely possible as tunnelling conditions appropriate for viewing the molecule are often bad for viewing the substrate and vice versa. Another interesting aspect is the origin of the observed molecular image contrast in STM. By varying the tunnelling conditions, one might expect to tunnel into selected molecular orbitals and image them. This is sometimes the case. However, the observed contrast is often rather robust over a wide bias voltage range, since the images originate from a superposition of individual molecular orbitals and substrate contributions [33, 34].

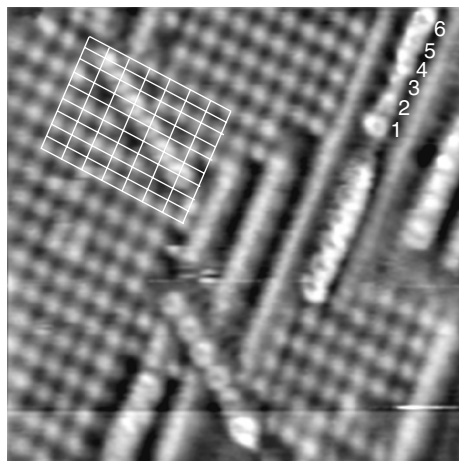


Fig. 1.7. Atomic scale image ($80 \times 80 \text{ \AA}^2$; 1.5 V, 0.1 nA) of individual sexiphenyl molecules. A (1×1) grid, where the corners match the underlying Ni(110) fourfold hollow positions, has been superimposed on the molecule in the top left corner (reprinted with permission from [33])

The major strengths of STM are the ability to determine the adsorption sites, the two-dimensional periodicity (even for very small domain sizes) and to evaluate changes to the substrate due to molecular adsorption.

A second technique that can evaluate the two-dimensional periodicity of the organic layer is low energy electron diffraction (LEED). While principally very accurate in determining the adsorbate periodicity, with most organic systems it faces the problem of severe damage under the beam of low energy electrons [35]. This can sometimes be improved by using very low electron beam currents or by cooling the sample.

1.4 Crystallographic Characterisation

While crystal structure investigations of inorganic nanoaggregates are frequently performed, organic nanoaggregates are much less studied. The experimental difficulties are small diffraction signals in case of X-ray diffraction and neutron diffraction. Surprisingly, neutron diffraction works for thin organic films [36]. The advantage of electron diffraction studies is the good sensitivity, however the degradation of the organic material due to the electron bombardment is a real problem.

X-ray diffraction studies of thin organic films also show some difficulties. The low scattering probability of the involved atoms (mainly carbon and hydrogen) together with the small scattering volume result in diffraction patterns with small intensities. However, thin films of molecular crystals show acceptable intensity which can be observed by standard laboratory equipment. In case of films with low crystallographic order and also for ultrathin films (with a thickness of few monolayers), synchrotron radiation has to be used. The low crystal symmetry (triclinic, monoclinic or orthorhombic) together with large lattice constants imply a huge number of diffraction peaks which are frequently overlapping.

Good results for structural characterisation of organic nanoaggregates are obtained by combining different diffraction techniques. X-ray diffraction has low sensitivity but high resolution regarding the reciprocal space. It can be combined quite nicely with transmission electron microscopy techniques which have high sensitivity with high spacial resolution. Supplementary information to the crystalline order is the morphology of the nanoaggregates; it can be obtained by diverse microscopy methods. In case of transmission electron techniques both, diffraction and microscopy, can be combined so that the morphology and the crystal structure properties can be related.

The main goals of crystallographic investigations are the determination of basic crystalline properties like crystalline phases, preferred orientations (or epitaxial orders) of crystallites and crystal sizes. The correlation of crystallographic order with the film morphology reveals basic information on the growth mechanisms of organic nanoaggregates on surfaces.

1.5 Fundamentals of Atomic Force Microscopy

AFM is nowadays the favoured imaging technique to investigate organic nanostructures because it is applicable under different environmental conditions and does not require conducting or semiconducting surfaces like STM does. Moreover, due to the imaging principle of AFM, where a sharp probe is scanned across the surface, the resulting image represents a three-dimensional topography $z_{ij} = z(x, y)$. Assuming a proper calibration of the piezoelectric scanner and an infinitely sharp AFM tip, the measured topography corresponds to the true three-dimensional topography of the investigated surface. In the real case of finite dimensions of the probe, the probe geometry has to be taken into account [37]. However, for lateral structure sizes that exceed the tip radius and structure slopes less than half of the opening angle of the AFM tip, this effect can be neglected. Thus, nanostructure size, three-dimensional shape and arrangement can be detected and quantitatively analysed [38]. Moreover, by analysing one-dimensional cross sections through an AFM image, z_{ij} , information on layer distribution and on step heights can be derived. For example, as will be shown in several chapters, terraces and island heights analysis in conjunction with corresponding crystallographic data (X-ray measurements) yields a worthwhile information about the orientation of organic molecules relative to the substrate surface (“lying-down” or “standing-up” growth in organic epitaxy). For three-dimensional islands, straight segments in the cross sections along certain directions reveal the existence of side facets. Analysing the histograms of orientations of local surfaces may yield not only orientation of the facets, but also quantitative information on their area fraction. With respect to self-organised, quasi-periodic structures, two-dimensional power spectrum formalism can be applied to the $z_{ij} = z(x, y)$ matrix, to deduce average real space orientation, symmetry and lateral periodicity of the surface pattern. All these AFM possibilities are of special importance for organic thin films growth, where additional degrees of freedom (orientational and vibrational) of extended organic molecules can result in a large variety of differently oriented three-dimensional morphological features. For further details concerning fundamentals of quantitative analysis of AFM measurements, the reader is referred to Chap. 2.2 of review paper [38].

As shown in Fig. 1.8, three different measurement modes can be generally realised during AFM depending on sample tip separation: contact (C), non-contact (NC) and intermittent contact (IC, often called also as *tapping* mode) modes. In contact mode, i.e. in the repulsive region of the van der Waals forces (at tip sample distances below 1 nm), the interaction between the tip and the surface results in the deflection of the cantilever (on which the interacting tip is mounted), which thus acts as a force sensor. A feedback loop keeps the static deflection constant by adjusting the vertical position of the cantilever base, providing a topographic image. In this mode scanning can be destructive for both the tip and the surface, which is especially true for soft organic samples. This limitation is circumvented in tapping mode AFM

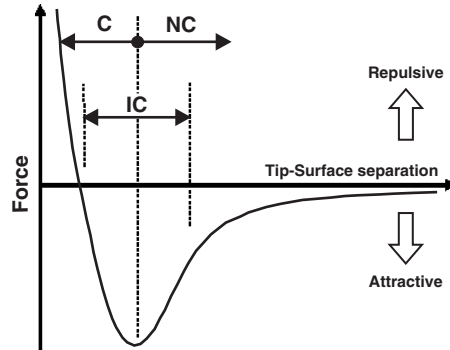


Fig. 1.8. Dependence of van der Waals force on tip sample separation. Contact (*C*), non-contact (*NC*) and intermittent contact (*IC*) modes are shown (reprinted with permission from [39])

(*IC* in Fig. 1.8). Here, the tip is mechanically oscillated close to its resonance frequency. On approaching the surface, the oscillation amplitude decreases and its phase changes due to the interaction with the surface. Most often the amplitude is then used as the detection signal and scanning is performed so that the oscillation amplitude is kept at predefined set point value smaller than the oscillation amplitude in free space. The phase shift can also be monitored. In this mode, the tip interacts with the surface most strongly in the lower part of the trajectory. Finally, in non-contact AFM (*NC-AFM*), the tip oscillates in the attractive region of the van der Waals forces and the resonant frequency shift of the cantilever measured by a phase lock loop is used as a feedback signal, providing true non-invasive imaging [41]. Note that high and even atomic resolution is possible in both contact mode AFM and *NC-AFM*. For further details concerning different variants of the AFM, the reader is referred to a recent paper [39].

One of the advantages of AFM tapping mode is that it allows to measure a phase contrast on the surface, which means that it is possible to distinguish between softer and harder surface areas [42]. Operating principle of such phase contrast imaging is shown in Fig. 1.9. The phase shift between the cantilever oscillating signal and the cantilever output signal from the split photodiode is monitored here simultaneously with topography while operating in tapping mode. As it can be seen in Fig. 1.9, a harder material induces consequently a much stronger phase shift than softer one, where the tip can penetrate a bit into the material, see also Fig. 11.15 in Chap. 11. As a consequence, the phase shift image reflects the changes in the viscoelastic properties of the sample surface [42]. However, in the practical use of this method, it can happen that morphological features with high and sharp edges can influence the phase measurements. Therefore, it is always needed to carefully compare corresponding phase and height images, to be sure that the detected phase contrast is not just a morphological artefact.

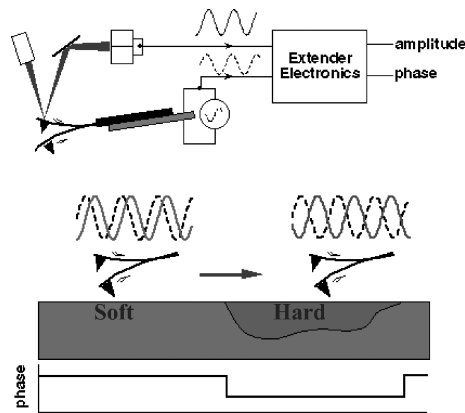


Fig. 1.9. Working principle of the phase shift imaging in tapping mode AFM (reprinted with permission from [40])

For further details concerning fundamentals of AFM measurements, the reader is referred to review papers [38,39].

References

1. F. Gutmann, L. Lyons, *Organic Semiconductors* (Wiley, New York, 1967)
2. M. Pope, C. Swenberg, *Electronic Processes in Organic Crystals and Polymers*, 2nd edn. (Oxford University Press, New York, 1999)
3. T. Mikami, H. Yanagi, *Appl. Phys. Lett.* **73**, 563 (1998)
4. F. Balzer, V. Bordo, A. Simonsen, H.G. Rubahn, *Appl. Phys. Lett.* **82**, 10 (2003)
5. N. Karl, *Charge-Carrier Mobility in Organic Crystals* (Springer, Berlin Heidelberg New York, 2003)
6. E. Silinsh, V. Capek, *Organic Molecular Crystals* (American Institute of Physics, New York, 1994)
7. J. Bredas, J. Calbert, D. de Silva, J. Cornil, *Proc. Natl Acad. Sci. USA* **99**, 5804 (2002)
8. J. Laquindanum, H. Katz, A. Lovinger, A. Dodabalapur, *Chem. Mater.* **8**, 2542 (1996)
9. G. Horowitz, M. Hjlouai, *Adv. Mater.* **12**, 1046 (2000)
10. M. Gebhart, *Crystal Growth: An Introduction* (North Holland, Amsterdam, 1973), Chap. Epitaxy, p. 105
11. G. Stringfellow, *Rep. Prog. Phys.* **45**, 469 (1982)
12. M.A. Herman, W. Richter, H. Sitter, *Epitaxy – Physical Principles and Technical Implementation, Springer Series in Material Sciences 62* (Springer, Berlin Heidelberg New York, 2004)
13. E.J. Kintzel, D.M. Smilgies, J.G. Skofronick, S.A. Safron, D.H.V. Winkle, *J. Cryst. Growth* **289**, 345 (2006)
14. S. Huefner, *Photoelectron Spectroscopy* (Springer, Berlin Heidelberg New York, 1995)

15. S.D. Kevan (ed.), *Angle-Resolved Photoemission* (Elsevier, Amsterdam, 1982)
16. E.W. Plummer, W. Eberhardt, *Adv. Chem. Phys.* **49**, 533 (1982)
17. H.P. Steinrück, *J. Phys.: Condens. Matter* **8**, 6465 (1996)
18. K. Jacobi, *Landolt-Börnstein (New Series)*, vol. 24 (Springer, Berlin Heidelberg New York, 1994), Chap. Electronic structure of surfaces, p. 56
19. R. Duschek, F. Mittendorfer, R. Blyth, F. Netzer, J. Hafner, M. Ramsey, *Chem. Phys. Lett.* **318**, 43 (2000)
20. M.G. Ramsey, D. Steinmüller, M. Schatzmayr, M. Kiskinova, F.P. Netzer, *Chem. Phys.* **177**, 349 (1993)
21. F.P. Netzer, M.G. Ramsey, *Crit. Rev. Solid State Mater. Sci.* **17**, 397 (1992)
22. J.P. Maier, D.W. Turner, *Faraday Discuss. Chem. Soc.* **54**, 149 (1972)
23. M.G. Ramsey, D. Steinmüller, F.P. Netzer, *J. Chem. Phys.* **92**, 6210 (1990)
24. G. Koller, F.P. Netzer, M.G. Ramsey, *Surf. Sci.* **421**, 353 (1999)
25. G. Koller, R.I.R. Blyth, S.A. Sardar, F.P. Netzer, M. Ramsey, *Surf. Sci.* **536**, 155 (2003)
26. D. Steinmüller, M.G. Ramsey, F.P. Netzer, *Phys. Rev. B* **47**, 13323 (1993)
27. G. Koller, S. Berkebile, J. Krenn, G. Tzvetkov, C. Teichert, R. Resel, F.P. Netzer, M.G. Ramsey, *Adv. Mater.* **16**, 2159 (2004)
28. B. Winter, S. Berkebile, J. Ivanco, G. Koller, F.P. Netzer, M.G. Ramsey, *Appl. Phys. Lett.* **88**, 253111 (2006)
29. M.G. Ramsey, F.P. Netzer, D. Steinmüller, D. Steinmüller-Nethl, D.R. Lloyd, *J. Chem. Phys.* **97**, 4489 (1992)
30. J. Stöhr, *NEXAFS Spectroscopy, Springer Series in Surface Sciences 25* (Springer, Berlin Heidelberg New York, 1992)
31. The Calculations Were Performed Using the StoBe (Stockholm Berlin 2005) Programm Package by K. Hermann, L.G.M. Pettersson, a Modified Version of the DFT-LCGTO Programm Package deMon by A. St.-Amant and D. Salahub (University of Montreal)
32. E.g. the SMART (Spectro-Microscope with Aberration Correction for Resolution and Transmission Enhancement) Project Stationed at the Synchrotron Radiation Facility BESSY II, Berlin
33. G. Koller, F.P. Netzer, M.G. Ramsey, *Surf. Sci. Lett.* **559**, L187 (2004)
34. P. Sautet, *Chem. Rev.* **97**, 1097 (1997)
35. B. Winter, J. Ivanco, F. Netzer, M.G. Ramsey, *Thin Solid Films* **433**, 269 (2003)
36. K. Herwig, J. Newton, H. Taub, *Phys. Rev. B* **50**, 15287 (1994)
37. J. Villarrubia, *J. Res. Natl Inst. Stand. Technol.* **102**, 425 (1997)
38. C. Teichert, *Phys. Rep.* **365**, 335 (2002)
39. S. Kalinin, R. Shao, D. Bonnell, *J. Am. Ceram. Soc.* **88**(5), 1077 (2005)
40. K.L. Babcock, C.B. Prater, Application Note AN11, Veeco (2004)
41. R. Albrecht, P. Grütter, D. Rugar, *J. Appl. Phys.* **69**, 668 (1991)
42. S.N. Magonov, V. Elings, M.H. Whangbo, *Surf. Sci.* **375**, L385 (1997)